# Palladium Nanohexagons and Nanospheres in Selective Alkyne Hydrogenation

**Natalia Semagina · Lioubov Kiwi-Minsker**

**Abstract** Palladium nanohexagons were prepared using a seed-mediated method. Their catalytic performance in 2-methyl-3-butyn-2-ol hydrogenation was compared to the one of monodispersed Pd nanospheres. Quantitative correlations between initial turnover frequencies (TOFs) and nanoparticle surface compositions showed independence of TOFs calculated per atoms on Pd(111) facets on particle size and shape.

**Keywords** Hydrogenation · Alkyne · Size effect · Shape effect · Pd-nanoparticle · AOT · CTAB

## 1 Introduction

The synthesis of metal nanostructures with controlled size and shape has attracted considerable attention in the past decade due to their size/shape-dependent properties [1–10]. For catalytic applications, much progress has been done in size effect studies for near spherical metal nanoparticles formed in the presence of a stabilizer [11–13] or on a heterogeneous support preventing their aggregation [14–16]. Due to a strict control over a metal nanoparticle growth in the presence of polymers [11, 12] or low molecular weight surfactants [13, 17], the catalytic behavior may be correlated

N. Semagina · L. Kiwi-Minsker (✉)
Group of Chemical Reaction Engineering, Ecole Polytechnique Fédérale de Lausanne, GGRC-EPFL, Station 6, CH-1015 Lausanne, Switzerland
e-mail: lioubov.kiwi-minsker@epfl.ch

*Present Address:*
N. Semagina
Department of Chemical and Materials Engineering, University of Alberta, Edmonton, Canada T6G 2G6

to the surface atom statistics. This allows revealing the reaction active sites. When the turnover frequencies (TOF) calculated per specific atoms (determined from surface statistics) do not change with the particle size, these atoms are considered as the active sites. Such reactions are supposed to be structure sensitive but size independent [16, 18] in a defined interval of particle diameters. In that way, size controlled synthesis of near spherical particles was used to determine the active sites for Suzuki [11] and Heck [12] coupling reactions.

Among structure-sensitive reactions, Pd-catalyzed hydrogenations of unsaturated carbon–carbon bonds are of special interest due to their importance in bulk and fine chemical production [19, 20]. First studies of liquid-phase 1-butyne hydrogenation over $Pd/SiO_2$ and $Pd/Al_2O_3$ revealed antipathetic size dependence of TOF calculated per total number of surface atoms [15]. Recently, 1,3-butadiene hydrogenation was studied over different $Pd/Al_2O_3/NiAl(110)$ model catalysts with Pd particle from 2 to 8 nm [16, 18]. TOFs normalized per number of Pd atoms within incomplete (111) facets were found not to change with the particle size above 4 nm. It was supposed that (111) facets are required for specific diene adsorption geometry. For the hydrogenation of allyl alcohol over dendrimer-encapsulated Pd nanoparticles, all terrace atoms were found to be the active sites for nanoparticles of 1.5–1.9 nm diameter [21].

Our recent studies of 2-methyl-3-butyn-2-ol hydrogenation over Pd near spherical nanoparticles of 6, 8, 11, and 13 nm diameter stabilized by AOT (sodium di-2-ethyl-hexylsulfosuccinate) in a reverse microemulsions showed the size independence of TOF calculated per Pd atoms within incomplete (111) facets [17]. So far, for structure sensitive hydrogenations a correlation of TOF with the number of specific surface atoms was performed either for unsupported near spherical or supported nanoparticles. Several recent

studies were devoted to catalytic behavior of different Pd nanostructures (rods, cubes, tetrahedrons) in hydrogenations [22, 23]. For example, in 1,3-butadiene hydrogenation TOF calculated per total surface atoms were found to vary with the shape and size of the nanostructures. This was explained by the presence of different crystallographic planes on the metal surface [23], however, no quantitative basis was provided. Presumably, Pd atoms on (111) facets should behave the same way regardless their belonging to any Pd structure, i.e., the structure sensitive hydrogenations should be not only size but also shape independent.

Here we report an experimental study of monodispersed Pd nanohexagons in 2-methyl-3-butyn-2-ol (MBY) catalytic hydrogenation to 2-methyl-3-buten-2-ol (MBE) [17]. There catalytic performance is compared to the one of Pd nanospheres [17] aiming at the quantitative correlation between the TOF and specific surface atoms of Pd nanostructures using crystal surface atom statistics [24]. Atoms on Pd(111) facets are demonstrated to be active sites independently on the nanoparticle shape and preparation conditions.

## 2 Experimental

### 2.1 Materials

Palladium (II) chloride (purum; *Fluka*), sodium borohydrate (98+%; *Acros Organics*), cetyltrimethylammonium bromide (purum, ≥96.0%; *Fluka*), ascorbic acid (puriss. p.a., ≥99.0%; *Sigma-Aldrich*), fumic hydrochloric acid (purum, p.a.; *Fluka*), nitric acid (puriss., p.a.; *Fluka*), 2-methyl-3-butyn-2-ol (purum, ≥99%; *Fluka*) and hydrogen (≥99.99% purity; *Carbagas*, Switzerland) were used as received. Demineralized–bidistilled water was used throughout this work.

### 2.2 Preparation and Characterization of Pd Nanohexagons

Preparation of Pd hexagons was carried out via a seed-mediating method as described for Au nanoobjects [25]. First, Pd near spherical nanoparticles of 4 nm diameter (seeds) were produced via the reduction of $H_2PdCl_4$ ($2.5 \times 10^{-4}$ M) by ice-cold $NaBH_4$ ($6.9 \times 10^{-4}$) in the presence of cetyltrimethylammonium bromide (CTAB, $7.5 \times 10^{-2}$ M). The $NaBH_4$ solution was added to the solution containing CTAB and Pd precursor, and the reaction mixture was then shaken for 2 min. The seeds were used within 24 h after synthesis for hexagon growth. Pd precursor solution was mixed with the CTAB solution for 5 min, then ascorbic acid was added as a week reductant of Pd precursor, and Pd seeds. The concentrations of CTAB, Pd seeds, Pd precursor and ascorbic acid in the

growth solution were $1.6 \times 10^{-2}$ M, $2.5 \times 10^{-6}$ M, $2.0 \times 10^{-4}$ M, and $6.0 \times 10^{-3}$ M, respectively. The colloidal dispersion was kept under weak stirring for 24 h.

To use the obtained nanostructures in the catalytic reaction, the colloidal dispersion was centrifuged at 10,000 rpm for 15 min. The precipitate was dispersed directly in the substrate of the catalytic reaction (MBY) under ultrasound. A part of the final solution was taken to analyze the Pd quantity. It was mixed with hot nitric acid, diluted with water and analyzed for Pd by atomic absorption spectroscopy (AAS) at 247.6 nm via a Shimadzu AA-6650 spectrometer with an air-acetylene flame.

Transmission electron microscopy (TEM) and energy-dispersive X-ray analysis (EDX) of the prepared nanostructures were carried out using a Philips CM 30 instrument at 300 kV, bright field images. Samples were prepared by ultrasonic dispersion of the precipitated during centrifugation nanostructures in water, their deposition onto the carbon film on the copper grid and evaporation in air at room temperature. More than 300 particles from different parts of the grid were used to determine the structure size and shape.

### 2.3 Catalytic Hydrogenation

Hydrogenations were carried out in a batch stainless steel reactor (100 mL autoclave, Buchi AG, Uster, Switzerland) equipped with a heating jacket, a hydrogen supply system, baffles and eight-blade disk turbine impeller. At the working temperature the reactor was filled with the reaction mixture and the catalyst, flushed with Ar and stirred for 10 min to equalize the temperature. Then the reactor was flushed with hydrogen and pressurized. During the course of the reaction, the pressure in the reactor was maintained constant. The experiments were carried out at 333 K and 0.28 MPa pressure at intensive stirring of 2,000 rpm. A total of 0.1 L (86.1 g) of 2-methyl-3-butyn-2-ol and 1.4 mg Pd were used rendering the substrate-to-Pd molar ratio of 72,000.

The samples were periodically withdrawn from the reactor and analyzed by GC as described elsewhere [17]. Values for the initial selectivity were obtained by extrapolation of selectivity-conversion dependence. As a measure of activity, initial TOF was used as $mol_{MBY} \, mol^{-1}_{Pd \, surface \, atoms} \, s^{-1}$ if not indicated otherwise. Initial TOF and selectivities were used since nanostructures may change their morphology during a catalytic reaction [6].

## 3 Results and Discussion

### 3.1 Pd Nanostructures

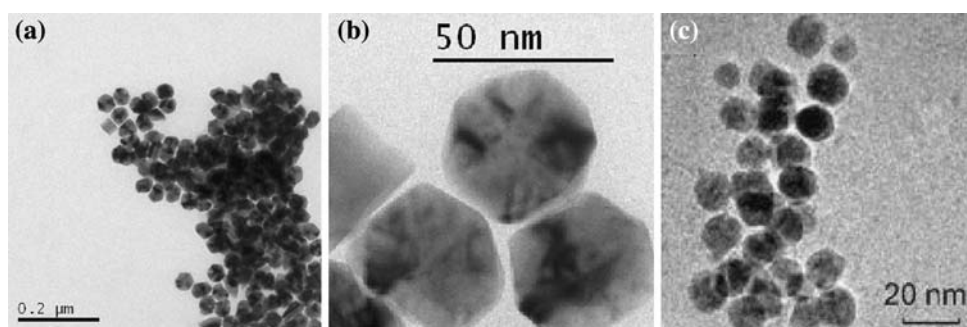TEM images of the synthesized Pd nanohexagons are presented in Fig. 1a, b. 95% of the nanostructures in the

**Table 1** Composition and characteristics of a "Pd nanohexagons" sample

| Shape of a nanostructure | Size[a], nm | Frequency (%) | D, %[b] | D$_S$, %[c] | D$_{111}$, %[d] |
|---|---|---|---|---|---|
| Hexagon | 21 ± 3 | 95 | 4.7 | 90 | 0.56 |
| Tetrahedron | 40 ± 3 | 1 | 9.4 | 1 | Negligible |
| Rod | 70 ± 10 × 25 ± 5 | 3 | 3.1 | 8 | 0.04 |
| Cube | 25 ± 2 | 1 | 3.9 | 2 | 0 |
| | | | Average: 4.5 | – | Average: 0.6 |

[a] Size for Pd nanostructures: for hexagons, tetrahedrons and cubes–length of a rib, for rods–(length) × (width)

[b] D is dispersion, surface atoms per total atoms in one nanostructure, %

[c] D$_S$ is a percentage of surface atoms of nanostructures of a definite shape with respect to all surface atoms in the catalyst, %

[d] D$_{111}$ is a percentage of atoms on (111) facets of the nanostructure with respect to all atoms in the catalyst, %

sample are hexagons with a rib length of 21 ± 3 nm, 5% are presented by tetrahedrons, rods and cubes as given in Table 1. Formation of the same shapes was reported for Au nanoparticles [25]. Similar hexagonal structures were recorded by TEM [26].

The formation of non-spherical shapes is known to be the outcome of the interplay between the faceting tendency of the stabilizing agent CTAB and the rate of supply of Pd$^0$ to the crystallographic planes grown from seeds [25]. CTAB is known to block selectively (100) facets so that the growth continues on free (111) facets [23, 25–28]. Here, CTAB concentration appears to be low and ascorbic acid concentration high enough to favor fast formation and deposition of Pd$^0$ onto the (111) facets, leading to their disappearance and the formation of (100) facets [25]. As a result, 95% of the obtained nanostructures were hexagons, which on TEM images correspond to hexagonal close packed crystals [29, 30] with a low content of (111) facets compared to face centered cubic crystals [24]. EDX analysis did not reveal chlorine presence from Pd precursor, while nitrogen was ascribed to cetyltrimethylammonium moiety stabilizing nanoparticles. Bromine ion was not detected in the sample, indicating that easy soluble Br$^-$ remained in the supernatant after centrifugation. Detailed structural characterization of anisotropic nanoparticles prepared via seed-mediated approach may be found elsewhere [30, and references herein].

Figure 1c (reprinted from [17]) shows a representative example of monodispersed Pd nanospheres prepared by a reverse microemulsion technique using AOT as a stabilizer [17].

### 3.2 Catalytic Performance

To estimate TOF, the surface atom statistics for each type of nanostructures composing the "Pd nanohexagons" sample was taken into account [24]. For hexagons, statistics of a truncated hexagonal bipyramid metal crystals was used knowing diameters of a Pd atom and of a nanoobject [24]. For tetrahedrons and cubes, the statistics of face centered cubic tetrahedron and cube was applied, respectively [24]. Rods exhibit predominantly (100) facets [23] similar to a cube, as well as (111) facets of a known size (width of a rod) similar to the facets of a tetrahedron. The cube and tetrahedron surface atom statistics were assumed to find dispersion for rods. The dispersions D (ratio of the surface atom to the total atom numbers) are presented in Table 1. The data allowed calculating the average dispersion D$_{av}$ for the "Pd nanohexagons" sample according to Eq. 1:

$$D_{av} = \frac{\sum_{i=1}^{n} \left( F_i \cdot N_i^{surface} \right)}{\sum_{i=1}^{n} \left( F_i \cdot N_i^{total} \right)} \cdot 100\% , \tag{1}$$
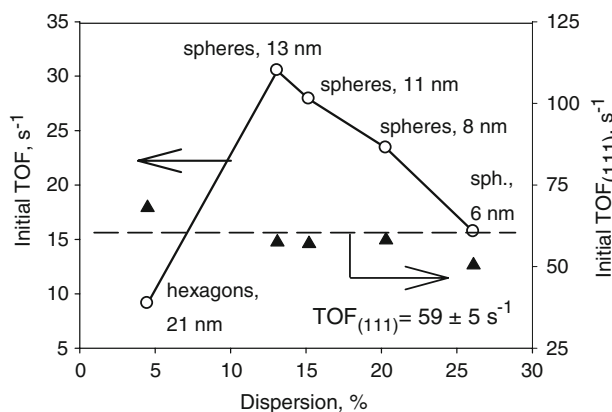
**Fig. 2** Size and shape dependences of TOF calculated per total surface atoms (initial TOF, left axis) and per atoms on Pd(111) facets (initial TOF$_{(111)}$, right axis) in 2-methyl-3-butyn-2-ol hydrogenation. Data for Pd6–Pd 13 are from [17]. Reaction conditions: 86.1 g MBY, 1.4 mg Pd, 333 K, 0.28 MPa, 2,000 rpm

where $i$ corresponds to the type of a nanostructure, $n$ is a total amount of types of nanostructures in the sample, $F$ is a frequency of each nanostructure in the sample, $N^{surface}$ and $N^{total}$ are the numbers of surface and total atoms in each nanostructure, respectively.

Initial TOF calculated using the average dispersion in MBY hydrogenation was found to be 9.1 s$^{-1}$ that is lower than for smaller Pd nanospheres (6–13 nm) stabilized by AOT [17], as shown in Fig. 2. The nature of a stabilizer may affect the nanoparticle performance, e.g., Pd nanoparticles of similar diameters, but stabilized by poly(vinylpyrrolidone) PVP or 1,10-phenanthroline, exhibited very different catalytic activities for the hydrogenation of 1,3-cyclooctadiene: a strongly interacting ligand like 1,10-phenanthroline, or tetraoctylammonium halide, can disturb the hydrogenation [32]. However, as we proposed earlier for MBY hydrogenation over AOT-stabilized Pd nanospheres [17], atoms on Pd(111) facets are the reaction active sites. In the case of hexagons, CTAB is known to block (100) facets [23, 25–28], which allows presuming that the Pd(111) atoms should behave similarly both on AOT- and CTAB-stabilized Pd nanostructures regardless their shape.

To verify this hypothesis, the dispersion of atoms on Pd(111) facets was calculated and used for TOF$_{(111)}$ determination. First of all, the percentage of surface atoms of each nanostructure with respect to all surface atoms in the sample was determined (Eq. 2) to understand which nanostructures govern the catalytic properties:

$$D_S = \frac{F_i \cdot N_i^{surface}}{\sum_{i=1}^{n} \left( F_i \cdot N_i^{surface} \right)} \cdot 100\% . \qquad (2)$$

Using the surface statistics [24], the number of atoms on (111) facets $N^{111}$ was calculated for each nanostructure and

used to estimate a percentage of atoms on (111) facets of the nanostructure with respect to all surface atoms in the sample (Eq. 3), value D$_{111}$ in Table 1):

$$D_{111} = \frac{F_i \cdot N_i^{111}}{\sum_{i=1}^{n} \left( F_i \cdot N_i^{total} \right)} \cdot 100\% . \qquad (3)$$

The dispersion of all atoms on (111) facets in the sample was calculated by summarizing the dispersions D$_{111}$ for each nanostructure (value "D$_{111}$ average" in Table 1).

Table 1 shows the calculated dispersions. The surface atoms of the sample are composed of 8% by the ones from the rods and of 90% by the ones from the hexagons. Cubes do not contain any (111) facets. Tetrahedrons are composed only of (111) facets but the percentage of surface atoms belonging to tetrahedrons with the respect to all surface atoms in the sample is low enough (1%) not to have an impact on the catalytic performance. As only 14% of surface atoms in a hexagon are the (111) facet atoms [24, 29, 30] as compared to 55% for spheres of 13 nm diameter, a low amount of Pd(111) facet atoms in the sample may be responsible for the lowest TOF among all the catalysts (Fig. 1).

As seen from Fig. 2, when TOF for the "Pd nanohexagons" sample was recalculated per number of (111) facet atoms as TOF$_{(111)}$, it was equal to the one of AOT-stabilized spheres of 6–13 nm diameter (59 $\pm$ 5 s$^{-1}$ with 10% RSD). Probably, the AOT and CTAB stabilizers do not block the (111) facet atoms for the adsorption of reactants, and the reaction takes place on these surface atoms. They are known to provide necessary adsorption geometry of the unsaturated substrate as proposed earlier for 1,3-butadiene hydrogenation [18]. Thus, MBY hydrogenation catalyzed by AOT- and CTAB-stabilized nanostructures is structure-sensitive and proceeds on the atoms located on (111) facets, independently on the shape and size of a nanostructure.

The initial selectivity to alkene MBE was found to be 96.2%, 95.9%, 96.2%, 96.1%, and 95.9% for hexagons and Pd spheres of 6, 8, 11, and 13 nm diameter, respectively. Given that the error in selectivity from six identical measurements is 0.1%, the selectivity is concluded to be structure independent that is in line with the studies of Pd catalysts in acetylene hydrogenation [33].

## 4 Conclusions

1. A Pd catalyst sample with 95% of nanohexagons with a rib length of 21 nm was prepared using a seed-mediated approach with CTAB as a stabilizer. The rest 5% was composed by rods, cubes and tetrahedrons.

2. The sample catalytic performance was studied in 2-methyl-3-butyn-2-ol hydrogenation and compared to

the one of Pd nanospheres of 6–13 nm diameter prepared by a reverse microemulsion technique using AOT as a stabilizer.

3. The crystal surface atom statistics for each type of a nanostructure in the "Pd nanohexagons" sample allowed calculating the number of total surface atoms and atoms located on (111) facets. The obtained dispersions were used to determine initial TOFs, which were found to be constant for atoms on (111) facets both for the "nanohexagons" sample and nanospheres of 6–13 nm size.

4. The MBY hydrogenation is thus supposed to be a structure-sensitive but intrinsically shape and size independent for AOT- and CTAB-stabilized nanostructures. The selectivity to alkene is structure-independent.

5. The highest TOF was observed on the particles with the highest amount of (111) planes which were the largest Pd spheres. Development of a nanostructure with predominant exposure of active sites is in progress.

# References

1. Burda C, Chen X, Narayanan R, El-Sayed MA (2005) Chem Rev 105:1025
2. Shchukin DG, Sukhorukov GB (2004) Adv Mater 16:671
3. Durand J, Teuma E, Gomez M (2008) Eur J Inorg Chem 23:3577
4. Pachon LD, Rothenberg G (2008) Appl Organomet Chem 22:288
5. Narayanan R, El-Sayed MA (2005) J Phys Chem B 109:12663
6. Narayanan R, El-Sayed MA (2005) Langmuir 21:2027
7. Sasaki M, Osada M, Higashimoto N, Yamamoto T, Fukuoka A, Ichikawa M (1999) J Mol Catal A 141:223
8. Balint I, Miyazaki A, Aika K (2004) Phys Chem Chem Phys 6:2000
9. Narayanan R, El-Sayed MA (2004) Nano Lett 4:1343
10. Narayanan R, El-Sayed MA (2004) J Phys Chem B 108:5726
11. Li Y, Boone E, El-Sayed MA (2002) Langmuir 18:4921
12. Le Bars J, Specht U, Bradley JS, Blackmond DG (1999) Langmuir 15:7621
13. Semagina N, Renken A, Kiwi-Minsker L (2007) J Phys Chem C 111:13933
14. Neri G, Musolino MG, Milone C, Pietropaolo D, Galvagno S (2001) Appl Catal A 208:307
15. Boitiaux JP, Cosyns J, Vasudevan S (1983) Appl Catal 6:41
16. Silvestre-Alberto J, Rupprechter G, Freund H-J (2006) J Catal 240:58
17. Semagina N, Renken A, Laub D, Kiwi-Minsker L (2007) J Catal 246:308
18. Silvestre-Albero J, Rupprechter G, Freund H-J (2006) Chem Commun 80
19. Molnar A, Sarkany A, Varga M (2001) J Mol Catal A 173:185
20. Chen B, Dingerdissen U, Krauter JGE, Rotgerink HGJL, Mobus K, Ostgard DJ, Panster P, Riermeier TH, Seebald S, Tacke T, Trauthwein H (2005) Appl Catal A 280:17
21. Wilson OM, Knecht MR, Garcia-Martinez JC, Crooks RM (2006) J Am Chem Soc 128:4510
22. Telkar MM, Rode CV, Chaudhari RV, Joshi SS, Nalawade AN (2004) Appl Catal A 273:11
23. Berhault G, Bisson L, Thomazeau C, Verdon C, Uzio D (2007) Appl Catal A 327:32
24. van Hardeveld R, Hartog F (1969) Surf Sci 15:189
25. Sau TK, Murphy C (2004) J Am Chem Soc 126:8648
26. Kumar S, Yang H, Zou S (2007) J Phys Chem 111:12933
27. Johnson CJ, Dujardin E, Davis SA, Murphy CJ, Mann S (2002) J Mater Chem 12:1765
28. Petroski JM, Wang ZL, Green TC, El-Sayed MA (1998) J Phys Chem B 102:3316
29. Walter J (2000) Adv Mater 12:31
30. Walter J, Shioyama H (1999) Phys Lett A 254:65
31. Bakshi MS, Sachar S, Kaur G, Bhandari P, Kaur G, Biesinger MC, Possmayer F, Petersen NO (2008) Cryst Growth Des 8:1713
32. Toshima N, Shiraishi Y, Teranishi T, Miyake M, Tominaga T, Watanabe H, Brijoux W, Bönnemann H, Schmid G (2001) Appl Organometal Chem 15:178
33. Borodzinski A (2001) Catal Lett 71:169